Effects of Angle of Attack on the Aerodynamic Performance of NACA 2412 Airfoil: Computational Fluid Dynamics Comparison of k-ε, k-ω, and k-ω SST Turbulence Models

Sainihal Reddy Nallappareddy

1. Abstract

The predictions of airfoil performance using computational fluid dynamics can be sensitive to the choice of turbulence model. The present study examined the effects of turbulence-model selection and angle of attack on the aerodynamic performance of a NACA 2412 airfoil. Eighteen simulations were run in SimScale with k-ε, k-ω and k-ω shear stress transport (SST) models at angles of attack from 0 to 10 degrees with 2 degree increments. All simulations were performed at a freestream velocity of 80 m/s and a Reynolds number of approximately 3.1E6. The models were validated in terms of lift coefficient, drag coefficient, lift to drag ratio, pressure and velocity contours and maximum y+ values. The most stable and accurate results were obtained using the k-ω SST model. The lift coefficient increased from 0.282 at 0° to 0.574 at 10°. This model underpredicted experimental lift values, but it produced the expected trend and predicted the highest aerodynamic efficiency among the models tested. The k-ω model also gave a generally consistent lift trend but predicted higher drag and lower aerodynamic efficiency. Conversely, the k-ε model was giving irregular and non-physical values at several angles of attack. These results demonstrate the importance of the turbulence model selection on the predicted airfoil performance and suggest that the k-ω SST was the most appropriate model for the conditions studied.

2. Introduction

Airfoils are used in aircraft because they generate lift and influence an aircraft's aerodynamic performance, which enables an airplane to fly. Airfoils are used because they create pressure differences between their upper and lower surfaces. Airfoils aren't just used in airplanes but also in wind turbines and helicopter rotors. The aerodynamic efficiency of the airfoil affects a machine's stability, performance, range, and energy consumption. The higher the aerodynamic efficiency, the better the performance and the lower the energy consumption. As air flows around the airfoil, the airflow in the upper camber accelerates, resulting in lower pressure. The pressure differences produce an upward force, lift, that lets an aircraft fly, while also producing drag, a force opposing motion and influencing a flight's efficiency, between the airfoil and the airflow.

One of the most important factors affecting airfoil performance is the angle of attack, the angle between the oncoming airflow and the airfoil chord. The angle of attack changes the flow around the airfoil. The simulated aerodynamics of the airfoil are also determined by the Reynolds Number, which is used to predict whether a fluid flows in a laminar manner (straight) or in turbulence (with swirls and vortices). This affects the lift and drag forces. As the angle of attack increases, the pressure difference across the camber increases, increasing the lift force. However, increasing the pressure difference also increases the drag force. At high angles of attack, airflow can separate from the upper surface of an airfoil, reducing lift and increasing drag. This concept is known as a stall.

Computational Fluid Dynamics (CFD) is a common tool for aerodynamic analysis, enabling researchers to explore airflow under a range of operating conditions without physical testing. CFD has become increasingly important over time because experiments, such as wind tunnel testing, can be expensive and time-consuming. CFD enables researchers to examine velocity and pressure contours and aerodynamic forces across multiple trials and variables. As a result, CFD has become a valuable tool for analyzing aerodynamics and airfoil performance. CFD is also a valuable tool because it allows researchers to visualize flow fields, such as pressure and velocity, enabling deeper investigations.

Additionally, CFD settings are relatively easy to change, so researchers can simulate flow over a geometry, such as an airfoil, under multiple conditions, such as a range of angles of attack. However, the accuracy of CFD simulations can vary depending on the turbulent flow modeling method. Different turbulence models estimate turbulence differently since turbulent flows around airfoils are complex. Therefore, selecting a single turbulence model is essential for collecting accurate data. Since each turbulence model makes different assumptions about flow behavior, there is no universal model suitable for all applications. Evaluating the capabilities of these models under identical conditions can improve understanding of their strengths and limitations and provide guidance for future CFD simulation studies. Thus, this study investigates the effect of angle of attack on the aerodynamics of a NACA 2412 airfoil by using CFD simulations. The study aims to evaluate how the choice of turbulence model influences the predicted aerodynamic performance of a NACA 2412 airfoil. By comparing the lift and drag coefficients and the lift-to-drag ratio across the k-ω, k-ε, and k-ω SST models at various angles of attack, this study aims to identify similarities and differences in their predictions and determine which turbulence model provides the most realistic aerodynamic predictions for the NACA 2412 airfoil.

3. Literature Review

This section reviews previous studies analyzing the NACA 2412 airfoil, CFD, and turbulence models. The topic includes the effects of angle of attack on lift and drag coefficients and aerodynamic efficiency, as well as the roles of turbulence models in CFD simulations for accurate predictions.

3.1 Mathematical Model

In the present work, the incompressible viscous flow around the spoiler is modeled using the RANS equation, which consists of the continuity equation and the momentum equation as follows:

$$\frac{\partial u_i}{\partial x_i} = 0$$

$$\frac{\partial(\rho u_i)}{\partial t} + \frac{\partial(\rho u_i u_j)}{\partial x_j} = -\frac{\partial P}{\partial x_i} + \frac{\partial}{\partial x_j}(\mu + \mu_t)\left(\frac{\partial u_i}{\partial x_j} + \frac{\partial u_j}{\partial x_i}\right)$$

All three turbulence models use them to calculate turbulent viscosity μ_t. Each model includes terms for transient behavior, convection, diffusion, turbulence production, and dissipation. However, the models differ in the variables they solve for and in how they treat the near-wall and free-stream regions.

3.1.1 K-ϵ Model

The k-ε model solves transport equations for turbulence kinetic energy, k, and its dissipation rate, ε. In general form, these equations are:

$$\frac{\partial(\rho k)}{\partial t} + \frac{\partial(\rho k u_i)}{\partial x_i} = \frac{\partial}{\partial x_j}\left[\left(\mu + \frac{\mu_t}{\sigma_k}\right)\frac{\partial k}{\partial x_j}\right] + G_k - \rho\varepsilon$$

$$\frac{\partial(\rho \varepsilon)}{\partial t} + \frac{\partial(\rho \varepsilon u_i)}{\partial x_i} = \frac{\partial}{\partial x_j}\left[\left(\mu + \frac{\mu_t}{\sigma_\varepsilon}\right)\frac{\partial \varepsilon}{\partial x_j}\right] + C_{1\varepsilon}\frac{\varepsilon}{k}G_k - C_{2\varepsilon}\rho\frac{\varepsilon^2}{k}$$

Here, G_k represents the rate of production of turbulent kinetic energy, while σ_k, σ_ϵ, $C_{1\epsilon}$, $C_{2\epsilon}$ are model constants. The k-ε model is commonly applied to fully turbulent free-stream flows but generally requires wall functions to model the near-wall region.

3.1.2 K-ω Model

The k-ε model solves the transport equations for turbulent kinetic energy, k, and the specific dissipation rate, ωε. In general form, these equations are:

$$\frac{\partial(\rho k)}{\partial t} + \frac{\partial(\rho k u_i)}{\partial x_i} = \frac{\partial}{\partial x_j}\left(\Gamma_k \frac{\partial k}{\partial x_j}\right) + G_k - Y_k + S_k$$

$$\frac{\partial(\rho \omega)}{\partial t} + \frac{\partial(\rho \omega u_i)}{\partial x_i} = \frac{\partial}{\partial x_j}\left(\Gamma_\omega \frac{\partial \omega}{\partial x_j}\right) + G_\omega - Y_\omega + S_\omega$$

In these equations, G_k and G_w represent turbulence production, Y_k and Y_w represent dissipation, and Γ_k and Γ_ω represent effective diffusivity. Unlike the k-ε model, the k-ω model has good performance near solid surfaces but can be sensitive to the specified free-stream value of ω.

3.1.3 K-ω SST Model

The K-ω model also solves equations for k and ω.

$$\frac{\partial(\rho k)}{\partial t} + \frac{\partial(\rho k u_i)}{\partial x_i} = \frac{\partial}{\partial x_j}\left(\Gamma_k \frac{\partial k}{\partial x_j}\right) + G_k - Y_k + S_k$$

$$\frac{\partial(\rho \omega)}{\partial t} + \frac{\partial(\rho \omega u_i)}{\partial x_i} = \frac{\partial}{\partial x_j}\left(\Gamma_\omega \frac{\partial \omega}{\partial x_j}\right) + G_\omega - Y_\omega + D_\omega + S_\omega$$

The SST formulation is different from the standard k-ω formulation near the airfoil surface and gradually transitions toward k-ε behavior in the free stream.

3.1.4 Comparison between Models

The transport terms for turbulence production, convection, diffusion, and dissipation are similar in the three models. The main difference between them is the variable used to describe the turbulence dissipation and the treatment of different flow regions. The k-ε model solves for epsilon and is more generally applicable to free-stream flow. The k-ω model solves for omega and gives improved near-wall treatment. The k-ω SST model combines these two approaches using blending functions and includes a cross-diffusion term, which allows for better modeling of the flow in the near-wall and free-stream regions. This difference is especially important for airfoil simulations with boundary-layer development and adverse pressure gradients.

3.2 Previous Investigations of the Effects of Angle of Attack on the Aerodynamics of the NACA 2412 Airfoil

A great deal of aerodynamic research on airfoils uses the NACA 2412 airfoil due to its cambered geometry and extensive documentation. The NACA 2412 airfoil has a maximum camber of 2% located at 40% of the chord length and a maximum thickness of 12% of the chord (Abbott & Von Doenhoff, 1959). Its aerodynamic traits, including lift, drag, and pressure distributions, have been extensively studied and validated across multiple conditions. Therefore, the NACA 2412 airfoil has become a widely used benchmark for validating CFD simulations and comparing aerodynamic performance across different methods and turbulence models (Abbott & Von Doenhoff, 1959).

Several studies have examined the aerodynamic performance of the NACA 2412 airfoil under realistic operating conditions. In a NASA study, researchers examined the airfoil at a Reynolds number of 3.1×10^6. The study reported that the lift coefficient increased from approximately -0.15 to 1.55 over an angle-of-attack range of -4° to 15°. The authors also observed flow separation at a 15 ° angle of attack, as evidenced by a decrease in the lift coefficient. These findings show that the angle of attack plays a major role in the aerodynamic performance and flow behavior around the NACA 2412 airfoil (NASA).

Researchers investigated angles of attack from 0° to 20°. They analyzed their effects on aerodynamic efficiency and found that the lift coefficient increased with increasing angle of attack. At the same time, the drag coefficient increased with greater inclination, altering the pressure distribution around the airfoil and causing flow separation (Akgümüş Gök & Alnimer, 2024). However, aerodynamic efficiency began to decrease even as lift continued to increase, as the airfoil stalled due to flow separation, disrupting smooth airflow (Akgümüş Gök & Alnimer, 2024). The research concluded that NACA 2412, among the airfoils in the study, was the better airfoil because it had higher lift-to-drag ratios across the investigated range of angles of attack, indicating higher aerodynamic efficiency in the study's experimental setup (Akgümüş Gök & Alnimer, 2024). These findings demonstrate that the angle of attack is a significant factor affecting aerodynamic performance, specifically the amount of lift and drag produced, as well as aerodynamic efficiency.

3.3 Computational Fluid Dynamics

Computational Fluid Dynamics (CFD) is a simulation tool used to test fluid mechanics concepts and predict aerodynamic behavior by solving equations of fluid motion. CFD is widely used in engineering because it allows researchers to evaluate performance without the expense and logistical challenges of physical experimental testing (Versteeg & Malalasekera, 2007). These simulations can evaluate pressure and velocity distributions and can investigate lift and drag coefficients under specific conditions.CFD relies on the Navier-Stokes equations, which govern the conservation of mass and momentum in fluids. To solve them, the simulation domain is divided into a mesh of numerous cells, sometimes millions. The equations are solved throughout the mesh to approximate fluid behavior around a geometry (Versteeg & Malalasekera, 2007). A mesh's quality is a critical factor in determining a simulation's accuracy to real-world conditions because it affects how thoroughly flow features are captured.

Mesh quality is important because pressure distributions, boundary layers, and regions of flow separation occur over small distances. So, a mesh that is too coarse could fail to capture velocity and pressure gradients accurately. In contrast, a refined mesh can significantly increase computational cost and simulation time, but be more accurate (Versteeg & Malalasekera, 2007). For this paper, an optimal mesh setting was used to balance simulation time and result accuracy, enabling simulations to be completed within a reasonable time. Additionally, trade-offs were considered between computational cost and simulation accuracy, including mesh refinements and mesh density. One advantage of CFD is the ability to visualize different values across a field as a contour. Researchers can visualize pressure contours, velocity distributions, and flow structures that are difficult to measure and visualize in a wind tunnel experiment. Additionally, CFD allows multiple conditions to be tested without requiring physical modifications to experimental equipment. However, CFD results are numerical approximations and must be validated against experimental data.

Validation is important because it establishes confidence and reliability in the simulation methodology and results. By comparing simulation-generated data with previous research, researchers can evaluate a simulation's accuracy in representing real-world aerodynamic behavior. This study validates its CFD results using NASA data. This is because trends in lift and drag coefficients across different angles of attack provide confidence in the simulation setup and its ability to represent real conditions. However, any significant discrepancies indicate limitations in the simulation setup, mesh quality, boundary conditions, or the turbulence model approach.

For this study, CFD was selected as the analysis method to examine the aerodynamics of the NACA 2412 airfoil at multiple angles of attack, while varying the turbulence model. The CFD was a more practical option than wind-tunnel testing because it does not require specialized equipment to get measured values and fewer resources than wind-tunnel testing; also, because it reduces the time for collecting data at one angle of attack, so in CFDs, more simulations can be done in a smaller amount of time than wind-tunnel testing.

3.4 Turbulence Models for Computational Fluid Dynamics

Turbulence modeling is a critical aspect of CFD because resolving turbulent flow structures requires computational resources beyond what is available for most studies. Consequently, Reynolds-Averaged Navier-Stokes (RANS) models are commonly used to approximate the effects of turbulence while maintaining reasonable computational efficiency (Wilcox, 2006). Different models use different mathematical formulations, leading to variations in results. So, turbulence model selection is an important consideration in aerodynamic simulations.

The k-ε turbulence model is widely used in engineering practices. The model solves equations for turbulent kinetic energy and the turbulent dissipation rate. Due to its low computational cost, the k-ε model has been widely applied; however, it may be less effective in situations with pressure gradients and flow separation (Launder & Spalding, 1974). Low computational cost is an advantage when running multiple CFD simulations at different angles of attack, as it makes the process more efficient overall.

The k-ω turbulence model solves two transport equations but uses the specific dissipation rate, improving accuracy in boundary layers and near solid surfaces, making it useful for external aerodynamics (Wilcox, 2006). Because forces are generated by pressure and shear stress along an airfoil surface, accurate near-wall flow behavior is important for calculating lift and drag. Accurate prediction of boundary layers influences drag and lift coefficient calculations by affecting the pressure and velocity gradients at the airfoil surface.

The k-ω Shear Stress Transport (SST) model shares characteristics with both the k-ω and k-ε models. Near solid boundaries, the model behaves like a k-ωmodel; farther away, it behaves like a k-ε model. This hybrid model was developed to improve predictions of flows with adverse pressure contours and flow separation (Menter, 1994). As a result, the k-ω SST model has become a commonly used turbulence model in aerodynamic studies involving airfoils and wings (Menter, 1994). A model that predicts flow separation is useful for studying airfoils at higher angles of attack, where the flow is more separated and must be accounted for when evaluating lift and drag. Previous studies have used the k-ω SST model and reported that it improves predictions of separated flows by combining the accuracy of the k-ω and k-ε models.

Flow separation becomes more likely as the angle of attack increases, because stronger pressure gradients develop and can cause the flow to detach from the airfoil surface. When flow separation occurs, lift generation can decrease while drag increases, resulting in a lower lift-to-drag ratio. The lower lift-to-drag ratio indicates reduced aerodynamic efficiency. So, a turbulence model's ability to predict flow separation can strongly influence its predicted aerodynamic performance.

Although the 3 turbulence models are commonly used in CFD, each uses a different mathematical approach to represent turbulent flow. These different approaches can lead to variations in predicted lift, drag coefficients, and lift-to-drag ratios even when all other settings are unchanged (Wilcox, 2006). Ultimately, comparing multiple turbulence models can provide insight into the sensitivity of CFD predictions to the choice of turbulence model. Before conducting simulations, it is important to consider which model is most likely to yield accurate results. Previous studies have frequently used the k-ω SST model due to its ability to capture both near-wall behavior and flow separation. However, k-ω and k-ε models remain widely used because of their efficiency and successful application in many engineering studies.

Evaluating multiple turbulence models under identical operating conditions enables researchers to determine whether results are strongly dependent on the turbulence model. If multiple models produce similar results, confidence in numerical predictions could increase because the observed trends are less likely to be artifacts of a single turbulence model. Substantial differences among model predictions may indicate that the choice of turbulence model plays an important role in determining aerodynamic efficiency.

3.5 Research Gaps and Study Goals

Although previous research has demonstrated that the angle of attack influences the aerodynamic performance of the NACA 2412 airfoil, differences in computational methodologies can lead to variations in results. Specifically, k-ω, k-ω SST, and k-ε turbulence models have been widely used in airfoil simulations. However, the simulations they are most useful for may vary depending on flow conditions and the objectives of a study. Additionally, several studies have examined differences in turbulence model results; only a few have evaluated how different turbulence model settings influence aerodynamic efficiency across a range of angles of attack. Therefore, this study uses CFD simulations with the k-ω SST, k-ε, and k-ω turbulence models to investigate the effects of angle of attack on the lift, drag, and lift-to-drag ratio of a NACA 2412 airfoil at a Reynolds number of 3.1e06, and to compare results across the different turbulence models with previous studies. As a result, the study provides additional CFD-based data regarding the aerodynamics of the NACA 2412 airfoil and the influence of turbulence models on CFD predictions.

4. Methodology

This section explains the specific simulation settings and decisions used in SimScale computational fluid dynamics simulations. The topic includes geometry and mesh creation, boundary conditions, and validation to ensure accurate results.

4.1 Airfoil Geometry and Computational Domain

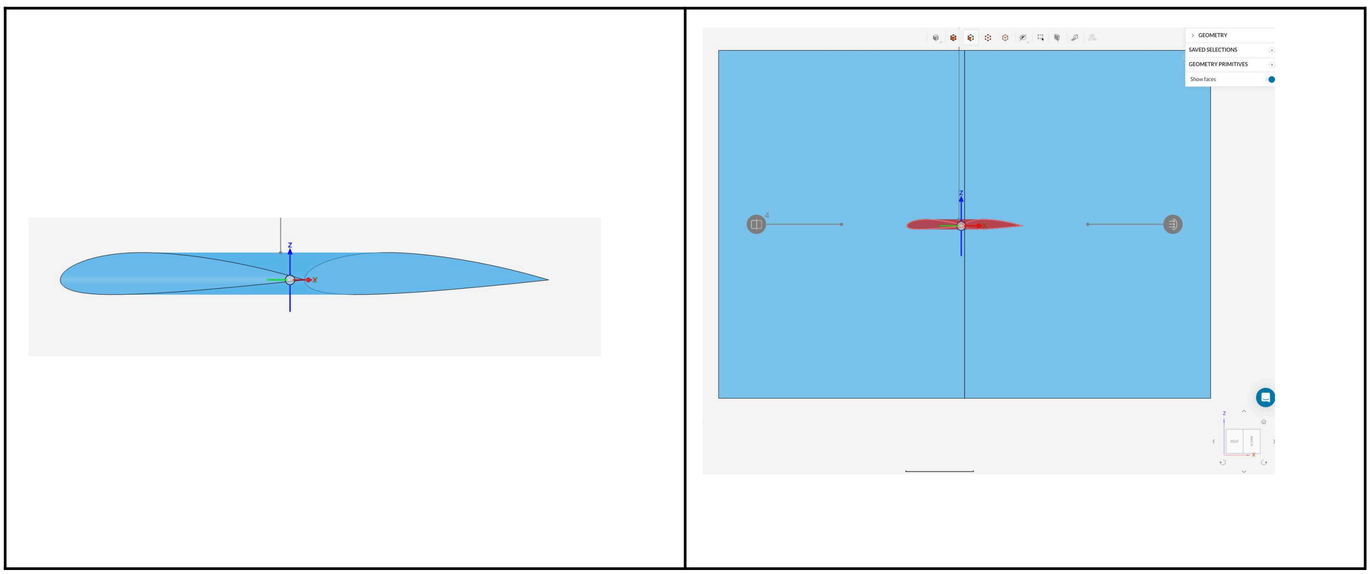

Figure 1. NACA 2412 Airfoil Geometry

The NACA 2412 airfoil was created as a sketch in Onshape, with a span of 0.60 and a chord length of 0.60m. The span was the length of the sketch's extrusion, 0.60m. The model was then imported into SimScale as a geometry for CFD analysis. The geometry was constant for all simulations. To ensure accuracy, the airfoil geometry was placed in a 3D external flow region that extended several chord lengths upstream, downstream, and perpendicular to the airfoil surface. This setup was designed to minimize the influence of the computational boundaries on the airflow.

4.2 Mesh Generation

An internal hex-dominant mesh was selected with automatic mesh sizing and automatic boundary layers enabled. The hex-dominant mesh was chosen because the hexagonal cells accurately capture the flow around the airfoil, thereby reducing numerical dissipation and improving solution accuracy compared to unstructured tetrahedral meshes. The finesse was set to the moderate setting in SimScale, producing 5.3E6 cells, based on grid-independent results from a k-ω model at an angle of attack of 0 degrees. The percentage errors in the table were calculated using the finest mesh as the reference value and the other mesh densities as approximations.

Cell Count	C_D	Percentage Error (%)	Airfoil Surface Mesh Image
4.3E6	**0.02920**	**0.409**	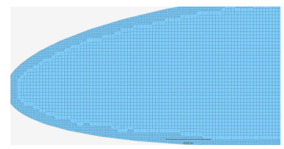
5.3E6	**0.02933**	**0.034**	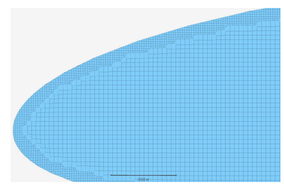
7.2E6	**0.02932**	**0**	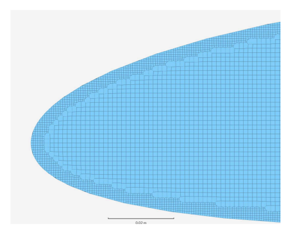

Table 1

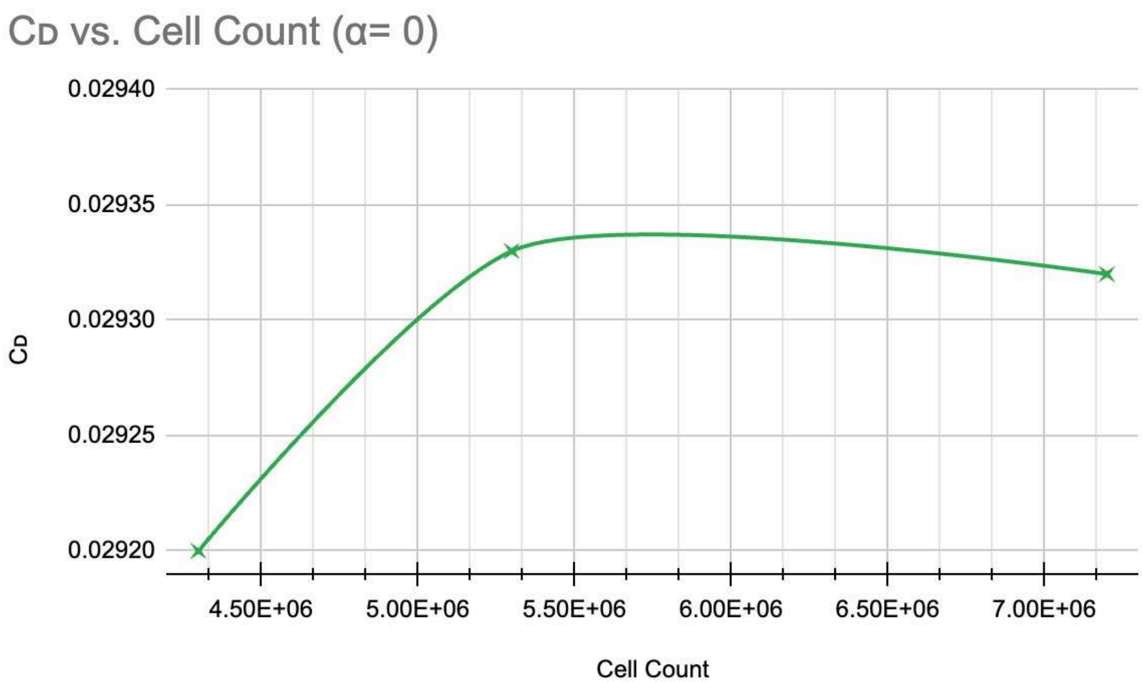

Figure 2. Drag Coefficient Versus Cell Count (Mesh-Independence Test)

4.3 Boundary Conditions

Air in the external flow region was modeled as an incompressible fluid with a density of 1.196 kg/m^3. The freestream velocity magnitude was set to 80 m/s to produce a Reynolds Number of approximately 3.1$\times 10^6$ based on airfoil chord length.

A velocity inlet condition was set with a magnitude and direction of 80 m/s in the negative x direction. To simulate a change in angle of attack, trigonometry was used to determine the magnitudes of the velocity components in the x and z directions, based on the desired angle of attack. The y direction was always kept at 0 m/s, the velocity value in x was set to negative, and the velocity value in the z direction was set to positive. A sample calculation of the velocity components for an angle of attack of 2 degrees is provided below. A pressure outlet of 0 Pa is specified at the downstream boundary. The airfoil surface was set as a no-slip surface. The wall boundary conditions were applied to the airfoil surfaces. In contrast, the symmetry boundary conditions were applied to the remaining outer surfaces of the computational domain to reduce artificial boundary effects.

Boundary	Boundary Condition Type	Specifications
Inlet	Velocity Inlet	Velocity Magnitude: 80 m/s
Inlet x-velocity	Velocity component	$V_x = V cos(\alpha)$
Inlet z-velocity	Velocity component	$V_z =- V sin(\alpha)$
Outlet	Pressure Outlet	Gauge Pressure: 0 Pa
Airfoil Surface	Wall	Stationary, No-slip wall
Top Boundary	Symmetry	Zero normal velocity
Bottom Boundary	Symmetry	Zero normal velocity
Side Boundaries	Symmetry	Zero normal velocity
Fluid Material	Air	Density: 1.196 kg/m^3
Operating Pressure	Pressure	101, 325 Pa

Table 2. Boundary Conditions and Simulation Specifications

4.4 Simulation Cases

Angles of attack of 0, 2, 4, 6, 8, and 10 degrees were simulated per turbulence model. Thus, 18 total simulations were conducted in the study. All simulations were run with identical boundary conditions, mesh settings, and flow conditions to ensure that differences in the results were attributable solely to the angle of attack and the turbulence model.

4.5 Validation Procedure

To verify the numerical setup, CFD predictions were compared with previous studies for the NACA 2412 airfoil at a Reynolds number of approximately 3.1e06. Validation was performed by comparing the lift and drag coefficients and the lift-to-drag ratio as a function of angle of attack. Percent errors were calculated between this and the previous numerical and experimental studies to evaluate the reliability of each turbulence model.

4.6 Aerodynamic Efficiency Performance

The lift and drag coefficients were used to calculate the lift-to-drag ratio; the higher the ratio, the greater the aerodynamic efficiency. Lift and drag coefficients were imported directly from the simulation results.

Additional flow visualizations, including pressure and velocity contours and y+ distributions, were used to examine flow behavior and explain differences among turbulence models. Y+ is a dimensionless parameter that corresponds to the distance of the first mesh cell from the wall. In this study, y+ values were analyzed to ensure that near-wall resolution was suitable for each turbulence model. Appropriate y+ values increase confidence in predictions of boundary-layer behavior, the lift coefficient, the drag coefficient, and wall shear stress.

5. Results and Discussion

This section will highlight the numerical results from the simulations conducted in this study, discuss their validation, and analyze pressure and velocity contours as evidence of aerodynamic efficiency and of differences between turbulence models.

5.1 Benchmark Comparison and Error Analysis

5.1.1 Validation for k-ω SST Against Data

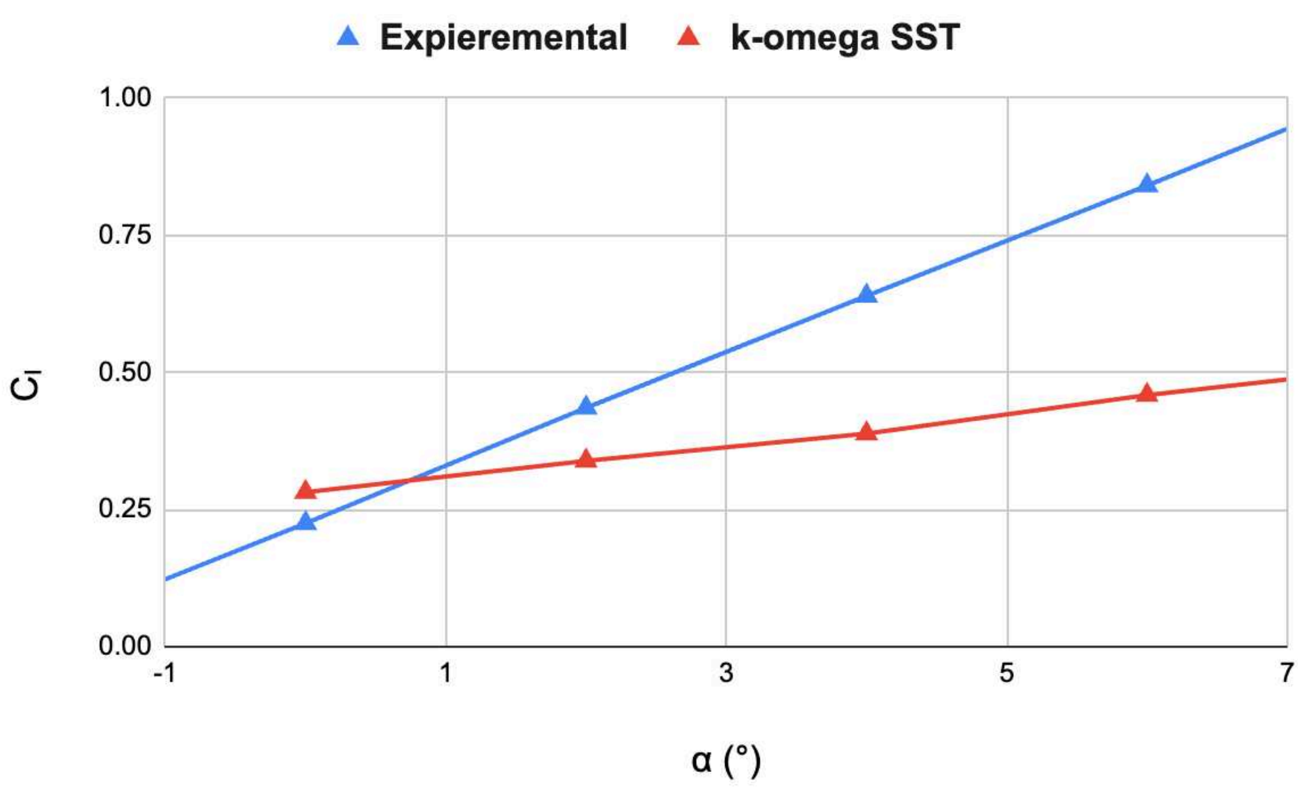

Figure 3. Comparison of k-ω SST Lift Coefficients with Experimental Data

Figure 3 compares lift coefficients predicted by the k-ω SST turbulence model with experimental data gathered from research by Abbott & von Deonhoff over angles of attack 0 to 10 degrees. The k-ω SST model was able to predict the general trend observed in the experimental data, that the lift coefficient increased with increasing angle of attack. The magnitude of the turbulence model showed a smooth, near-linear increase in the lift coefficient over the range studied, indicating stable, physically consistent aerodynamic behavior.

While the k-ω SST consistently underestimated the experimental lift coefficients, it preserved a stable lift curve for the tested range. The difference between the results increased with increasing angle of attack. In other words, the lift coefficients from the experiment grew faster than the CFD predictions. Even with this difference, the k-ω SST turbulence model was selected as the better model for the aerodynamic comparisons performed in this work, because of its numerical stability and ability to reproduce the general trend of the lift coefficient.

5.1.2 Validation for k-ω Model

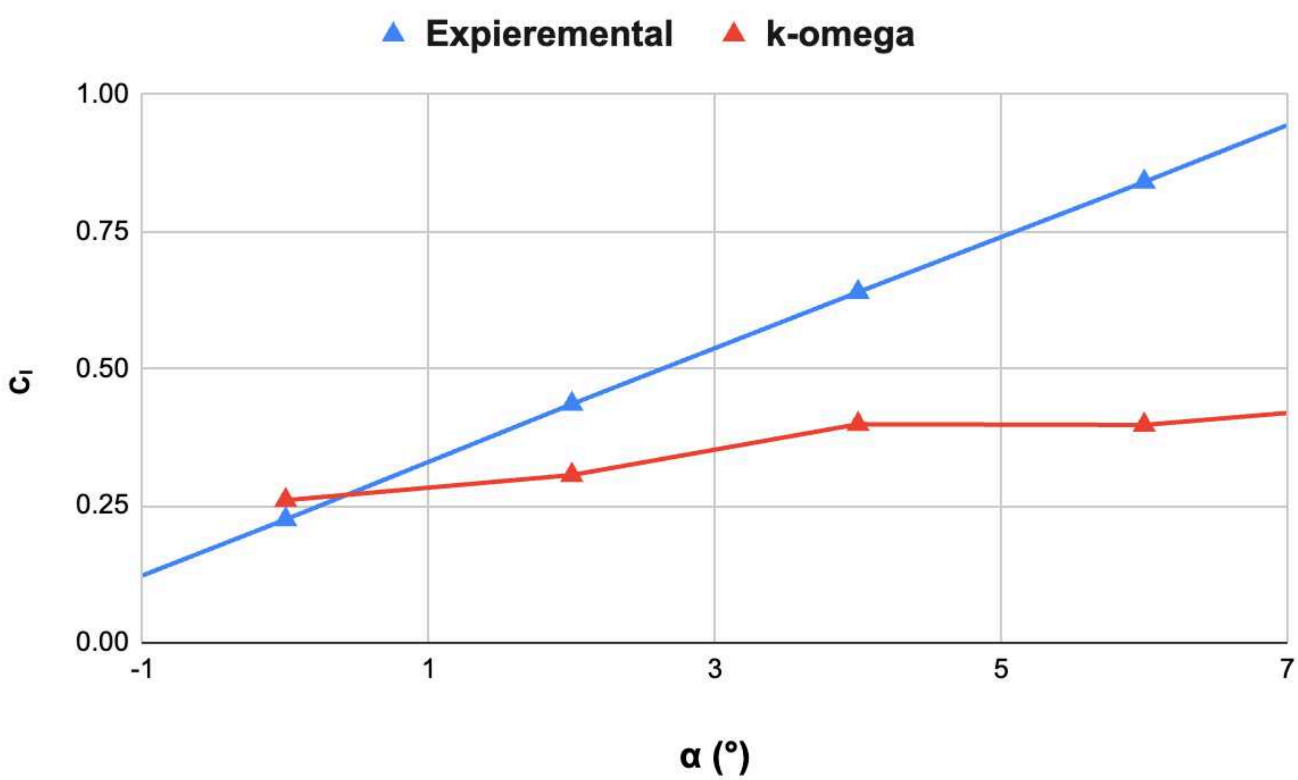

Figure 4. Comparison of k-ω Lift Coefficients with Experimental Data

Figure 4 compares lift coefficients predicted by the CFD simulations using the k-ω turbulence model with experimental data gathered from Abbott & von Doenhoff over the tested angle of attack range. The k-ω model captured the general trend of increasing lift coefficient with increasing angle of attack and produced realistic, stable results across the entire angle-of-attack range. At 0 degrees, the simulation predicted a slightly higher lift coefficient than the experimental value. However, at higher angles of attack, the model always underpredicted the lift coefficient.

The difference between the simulation and experimental lift coefficients became more pronounced as the angle of attack increased. The experimental data presented a linear increase in the lift coefficient. The k-ω predictions were more gradual and started plateauing at higher angles of attack, starting at 4 degrees. This behavior led to increasingly conservative lift predictions relative to experimental values. The k-ω can reflect the overall aerodynamic trend, but the agreement between the experimental value and the k-ω model is not as good as that of the k-ε SST model.

5.1.3 Validation of the k-ε Model

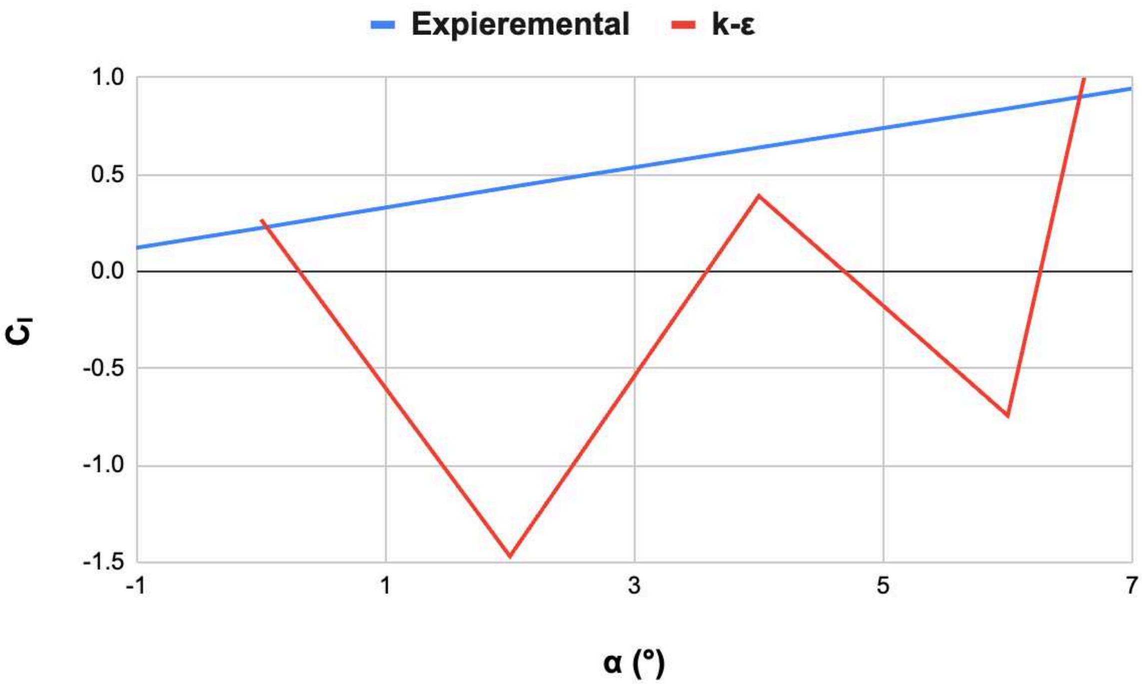

Figure 5. Comparison of k-ε Lift Coefficients with Experimental Data

Figure 5 depicts a comparison of the lift coefficients predicted by the k-ε turbulence model with the experimental data given by Abbott & von Deonhoff over the tested range of angles of attack. The k-ε did not accurately reproduce the lift coefficient trend over the tested range of angles of attack, while the k-ω SST and k-ω models did. The simulation at 0 degrees yielded a lift coefficient close to the experimental result; the other simulations showed significant discrepancies with the experimental data. The simulated lift coefficients exhibit a pronounced increase with increasing angle of attack, producing both negative and large positive values that are inconsistent with the expected aerodynamic behavior of a NACA 2412 airfoil.

The k-ε model produced several nonphysical predictions, even when using the same computational geometry, mesh, boundary conditions, solver settings, and simulation setup as the other turbulence models, indicating poor performance relative to the experimental data. These results show that the k-ε model did not consistently predict the lift characteristics of the NACA 2412 airfoil under the conditions studied.

One possible reason for poor performance is its reliance on wall-function formulations, which are very sensitive to near-wall mesh resolution and, consequently, y+ values. If the boundary-layer mesh is not appropriate for the wall functions, the model will yield inaccurate predictions of wall shear stress and pressure distribution, which will, in turn, affect the lift coefficient computed by the CFD. The k-ε model is also generally less successful in predicting flows with adverse pressure gradients and boundary-layer separation, both of which may become more important as the angle of attack increases. These limitations may have resulted in the large deviations and nonphysical lift coefficients observed in the k-ε model results.

5.2 Lift Coefficients

α (°)	k-ω SST	k-ω	k-ε
0	0.282	0.260	0.269
2	0.339	0.306	-1.469
4	0.388	0.399	0.390
6	0.459	0.397	-0.743
8	0.516	0.441	4.937
10	0.574	0.482	0.547

Table 3

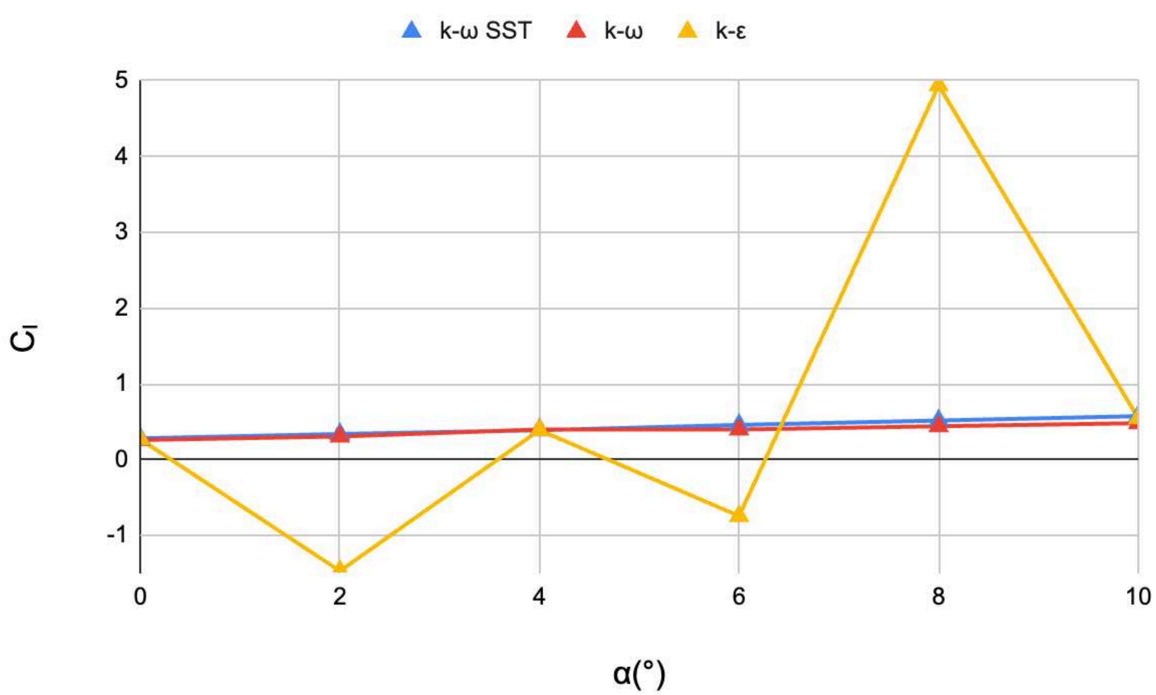

Figure 6. Lift Coefficient Versus Angle of Attack for the Three Turbulence Models

Table 3 and Figure 6 show a comparison of lift coefficients predicted by the k-ε, k-ω, and k-ω SST turbulence models over the investigated range of angles of attack. For both the k-ω SST and k-ω, the lift coefficient was predicted to increase gradually with angle of attack from 0 to 10 degrees, which is in agreement with the expected aerodynamic behavior of the NACA 2412 airfoil. The k-ω SST model predicted the highest lift coefficients, which increased from 0.282 at 0 degrees to 0.574 at 10 degrees. The k-ω was similar but yielded smaller lift coefficient magnitudes in the tested range.

The k-ε model, on the other hand, showed inconsistent, nonphysical behavior. The simulations at 0, 4, and 10 degrees yielded lift coefficients that were in good agreement with those of other models. The simulations at 2, 6, and 8 degrees produced nonphysical results: negative lift coefficients at 2 and 6 degrees, and a large positive lift coefficient at 8 degrees. Such irregular predictions are far from the trends of both k-ω models. Overall, the k-ω SST model provided the most stable and physically consistent predictions of the lift coefficient over the considered angle-of-attack range.

5.3 Drag Coefficients

α (°)	k-ω SST	k-ω	k-ε
0	0.016	0.069	0.051
2	0.025	0.077	0.156
4	0.036	0.037	0.058
6	0.053	0.102	0.130
8	0.071	0.120	0.180
10	0.092	0.139	0.110

Table 4

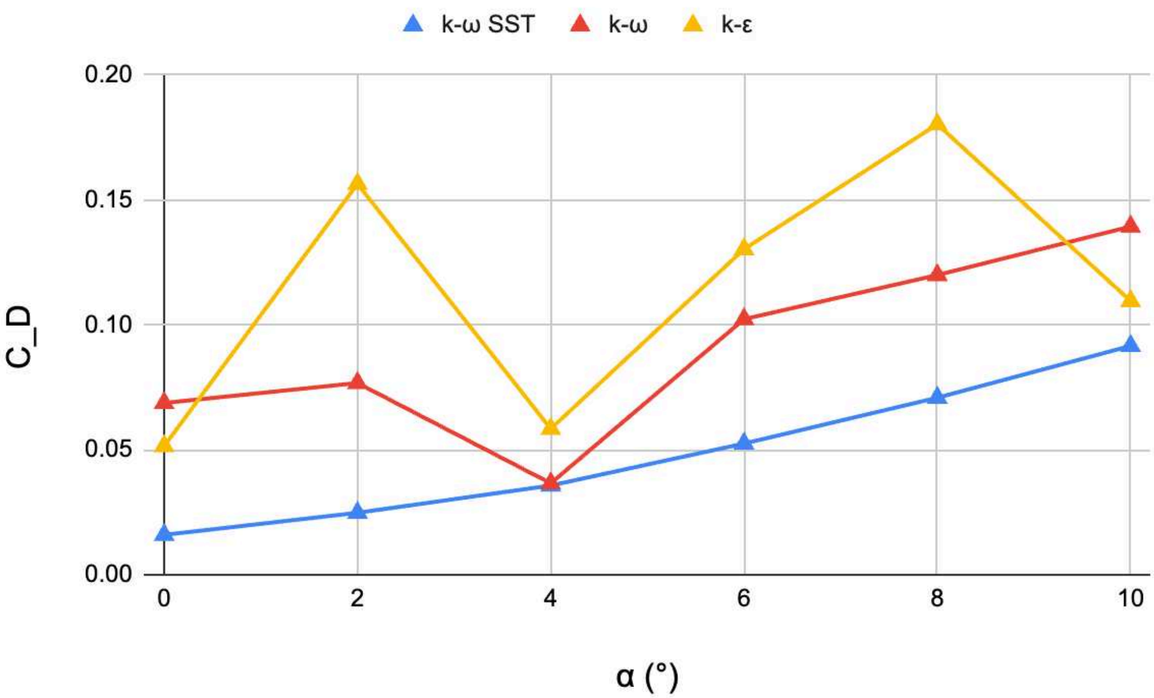

Figure 7. Drag Coefficient Versus Angle of Attack for the Three Turbulence Models

Table 2 and Figure 7 compare the drag coefficients predicted by the k-ω SST, k-ω, and k-ε models over the tested range of angles of attack. The drag coefficients were lowest for the k-ω SST at all angles of attack, of 0.016 at an angle of attack of 0 to 0.0912 at an angle of attack of 10 degrees, which is consistent with the expected aerodynamic performance of the NACA 2412 airfoil as higher angles of attack increase drag and pressure flow.

The k-ω predicted higher drag coefficients than k-ω SST at almost all angles of attack. The trend remained largely consistent in terms of physical behavior, but the drag coefficient increased more rapidly with angle of attack, reaching 0.139 at 10 degrees. The k-ω model predicted a reduction of the drag coefficient at 4 degrees before it increased again at higher angles of attack. The decrease was not in line with the increasing trend but was physically reasonable given the larger fluctuations with the k-ε model. The k-ε model yielded the least consistent drag predictions, with sharp changes in drag as a function of angle of attack. For example, the drag coefficient increased sharply at 2 degrees, decreased at 4 degrees, and then increased again at higher angles of attack. These differences are consistent with deviations in the lift coefficient from the k-ε model and further suggest that the k-ε model was unable to consistently predict the aerodynamic performance of the NACA 2412 airfoil under the conditions considered

5.4 Lift-to-Drag Ratio

α (°)	k-ω SST	k-ω	k-ε

0	17.65	3.78	5.22
2	13.67	3.99	-9.39
4	10.88	10.89	6.68
6	8.73	3.88	-5.70
8	7.28	3.68	27.39
10	6.27	3.46	5.00

Table 5

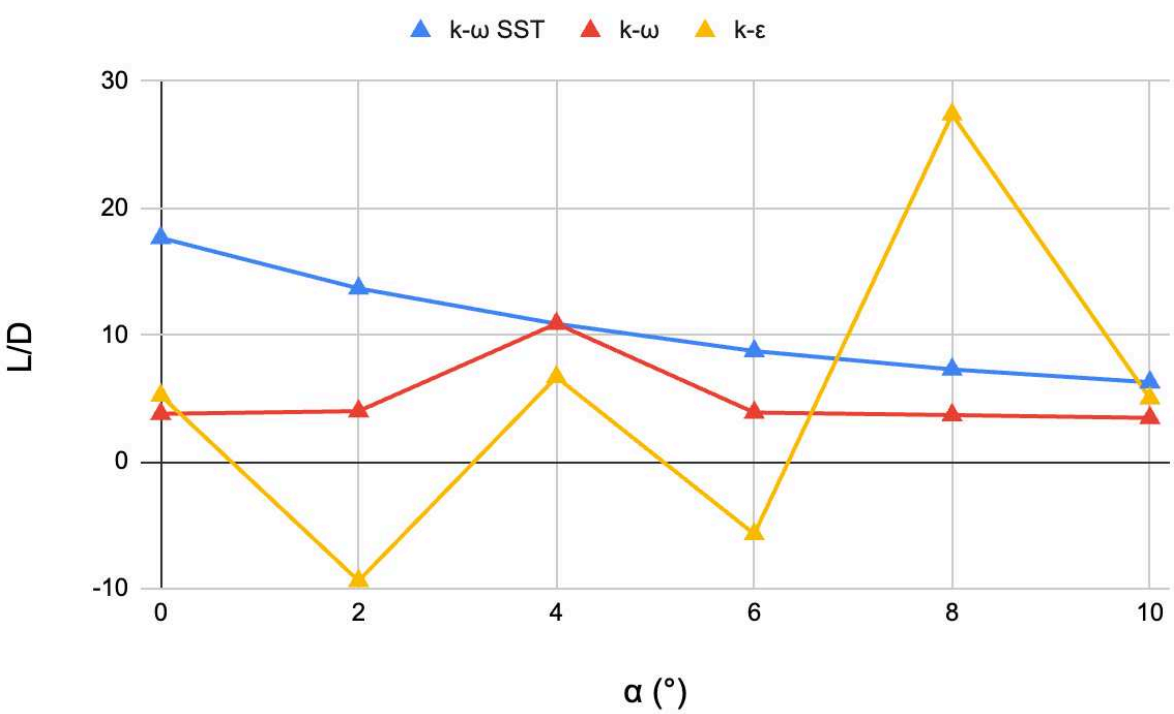

Figure 8. Lift-to-Drag Ratio Versus Angle of Attack for the Three Turbulence Models

Table 3 and Figure 8 show the predicted lift-to-drag ratio (L/D) over the investigated range of angles of attack using the k-ε, k-ω, and k-ω SST models over the investigated range of angles of attack. The k-ω SST model had the highest L/D, indicating the best aerodynamic efficiency. The L/D ratio decreased steadily from 17.65 at 0 degrees to 6.27 at 10 degrees, indicating increasing drag with increasing angle of attack. Although there was a gradual decrease, the k-ω model still provided higher aerodynamic efficiency than the other turbulence models.

The k-ω model gave significantly lower lift-to-drag ratios than the k-ω SST. These ratios were fairly constant between approximately 3.5 and 4.0, except for an increase at 4 degrees, which was due to a temporary decrease in the predicted drag coefficient. The k-ε model, however, was very erratic, with negative values at 2 and 6 degrees and an abnormally large positive value at 8 degrees. These results are consistent with the irregular lift and drag predictions discussed in previous sections and suggest that the k-ε model couldn't deliver accurate and consistent predictions of aerodynamic efficiency under the conditions investigated.

5.5 Flow Field Analysis

Turbulence Model	Pressure Contour (AoA 10)
k-ω	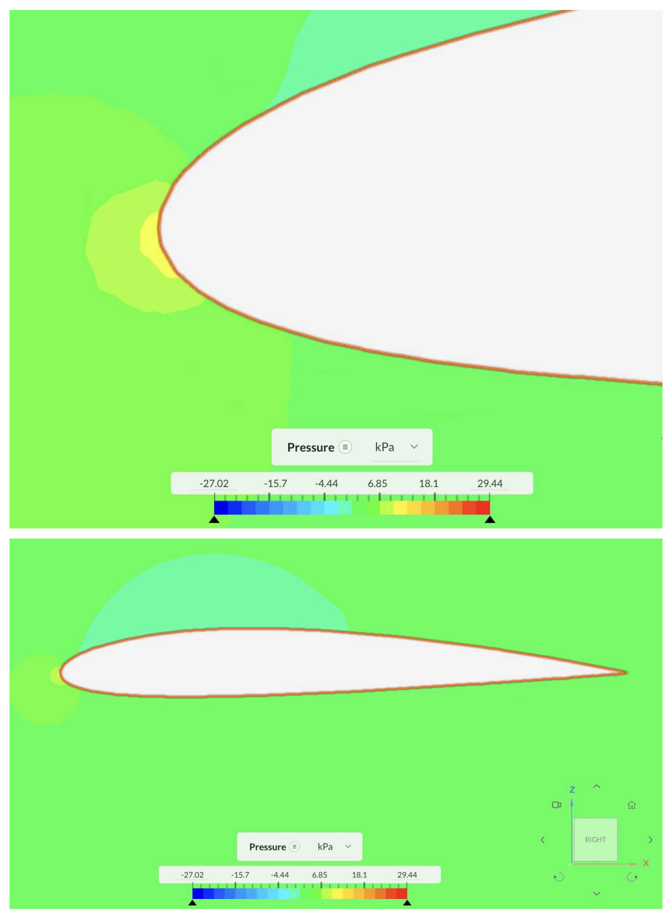

<table>
<tr><td>k-ω SST</td><td>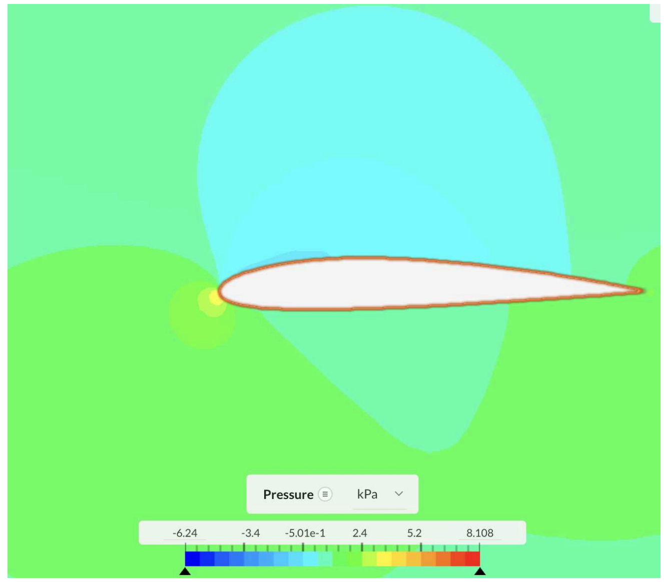

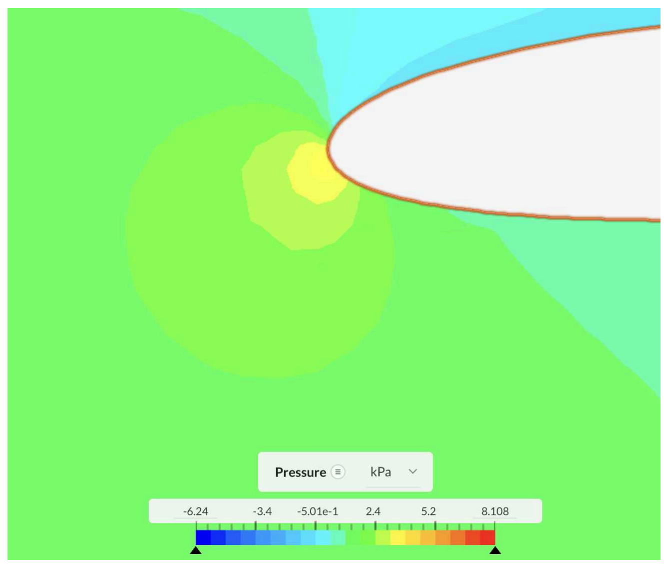
</td></tr>
</table>

k-ε	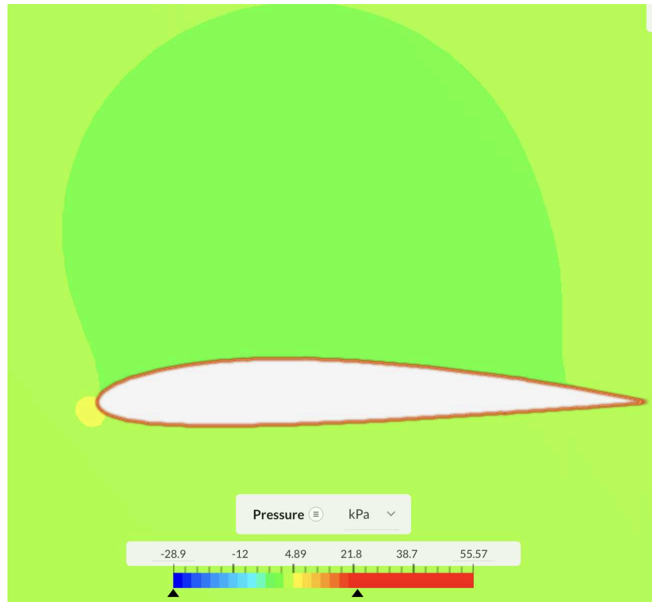 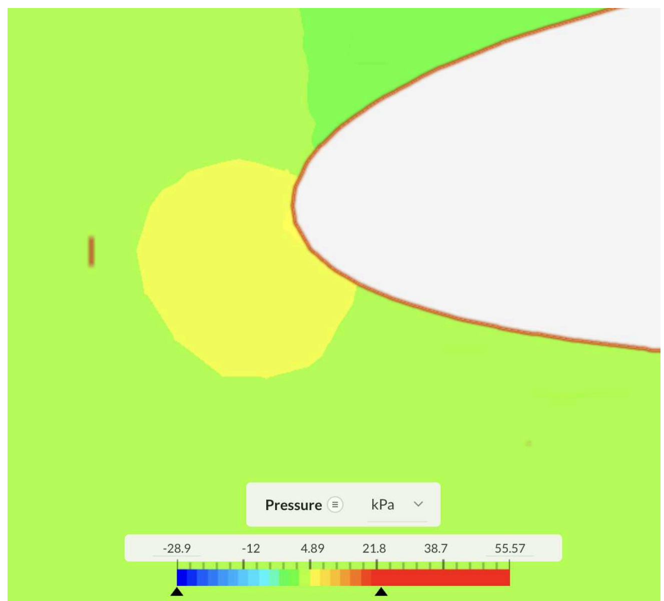

Table 6. Pressure Contours at an Angle of Attack of 10 Degrees

Table 6 presents the pressure contours predicted by the three turbulence models at an angle of attack of 10 degrees. For the pressure contours at an angle of attack of 10 degrees, all three turbulence models showed the presence of a region of high pressure at the stagnation point of the leading edge and region of low pressure on the upper surface of the airfoil. The k-ω SST model showed the most extensive and smoothest low-pressure region above the airfoil, indicating an organized pressure contour, which gave a higher value of lift coefficient prediction. For the k-ω turbulence model, there was a similar pressure contour, but the change in pressure was localized around the leading edge. The k-ε turbulence model had a much broader pressure range, going from about -28.9 kPa to 55.6 kPa compared with -27.0 kPa to 29.4 kPa for k-ω and

-6.24 kPa to 8.11 kPa for k-ω SST. This broad range explains the variation found for lift and drag coefficients of the k-ε model. Since each contour had a different default scale, the models were compared based on the position and shape of the pressure region and the numerical values indicated by the legends of the respective contours..

Velocity Contour Table (AoA 10)

k-ω	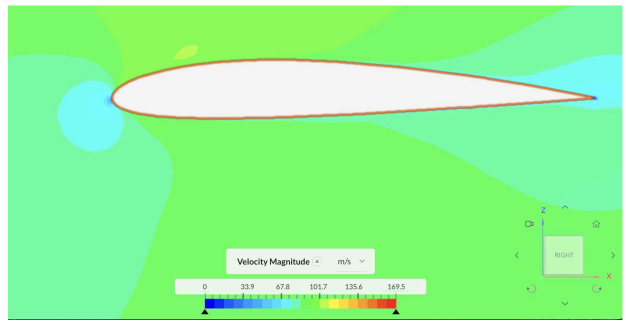
	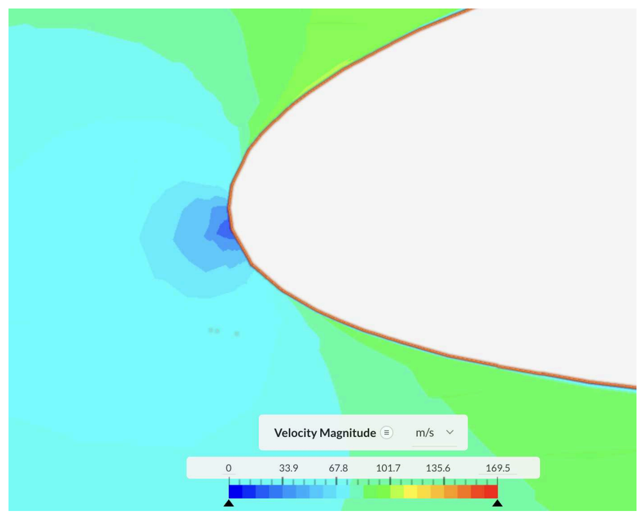

<table>
<tr><td></td><td>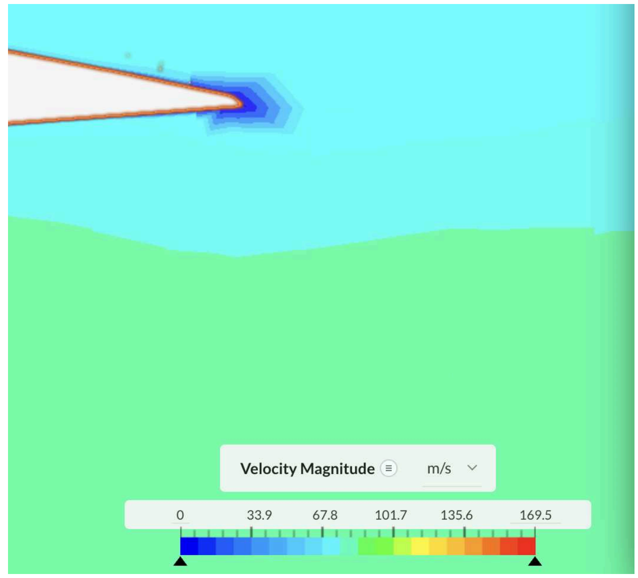
</td></tr>
</table>

<table>
<tr><td>k-ω SST</td><td>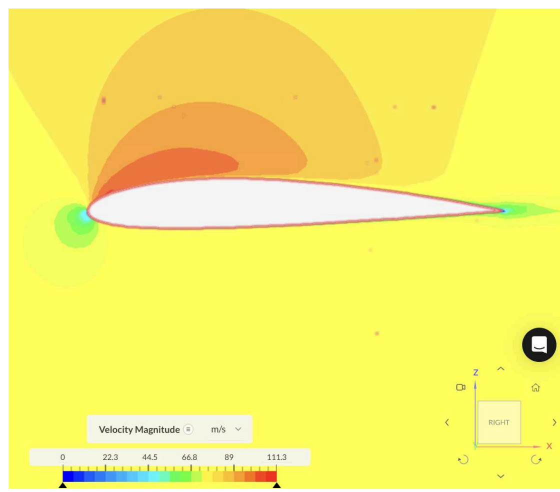
</td></tr>
</table>

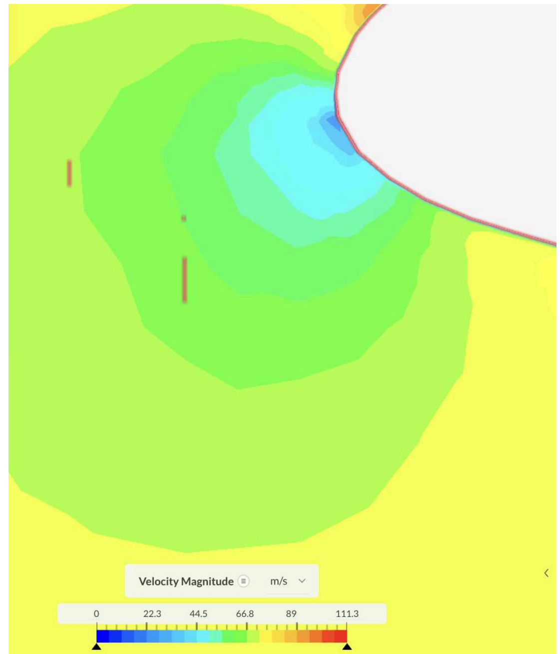
Velocity Magnitude
m/s
0
22.3
44.5
66.8
89
111.3

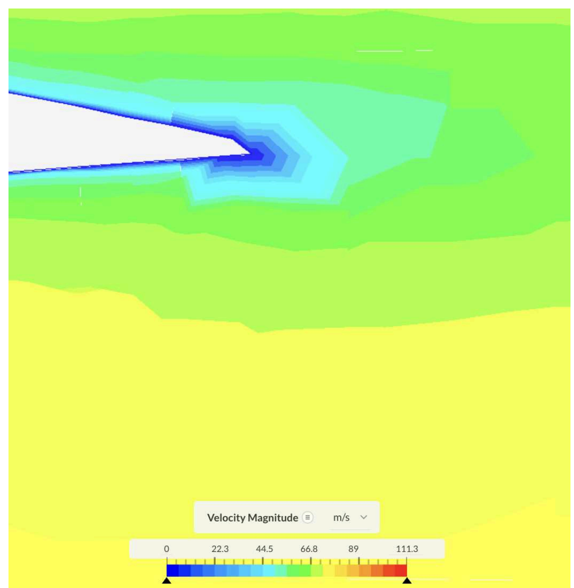
Velocity Magnitude
m/s
0
22.3
44.5
66.8
89
111.3

k-ε	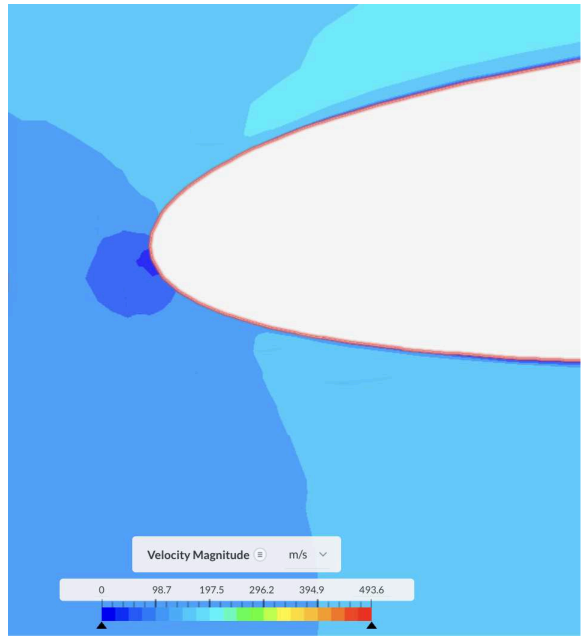Velocity Magnitude m/s 0 98.7 197.5 296.2 394.9 493.6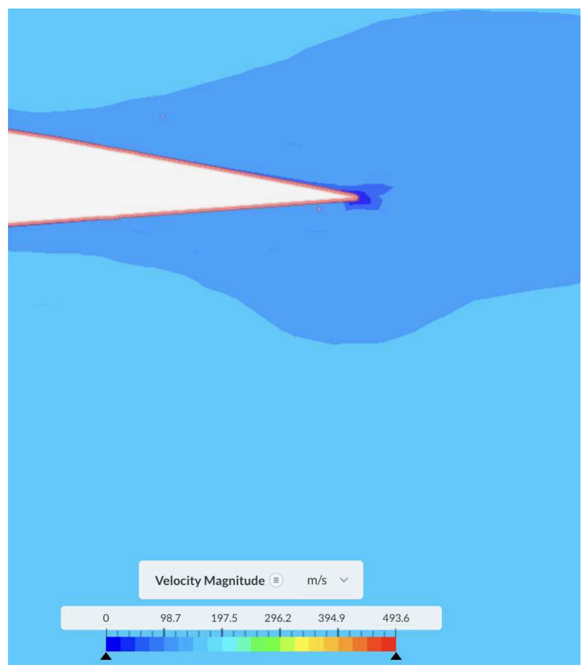Velocity Magnitude m/s 0 98.7 197.5 296.2 394.9 493.6

	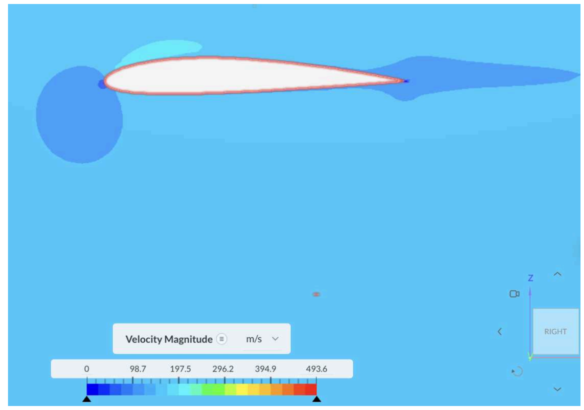

Table 7. Velocity Contours at an Angle of Attack of 10 Degrees

Table 7 presents the velocity contours predicted by the three turbulence models at an angle of attack of 10 degrees.The velocity contours at angle of attack of 10 degree shows acceleration over upper surface and low velocity regions near the leading edge and in the wake behind the trailing edge. The k-ω SST model exhibited a nearly smooth acceleration region over the upper surface and a well-defined low-velocity wake, indicating an organized flow pattern around the airfoil. The k-ω model also produces a similar overall pattern, but with a more localized low-velocity region near the leading edge and a narrower wake downstream. The k-ε contour, however, used a velocity range of up to about 493.6 m/s, which is much larger than the freestream velocity of 80 m/s and the maximum ranges shown for the other models. This wide range, along with the modified wake pattern, supports the conclusion that the k-ε simulation produced less consistent flow predictions under the tested conditions. The contours have different default scales, and so their colors were interpreted using the numerical legend of each image, rather than compared across models.

Turbulence Model	**Maximum Y+ (AoA 10)**
k-ω	**282.6**
k-ω SST	**272.2**
k-ε	**343.1**

Table 8. Maximum y+ Values at an Angle of Attack of 10 Degrees

Table 8 compares the maximum y+ values predicted at 10 degrees angle of attack with three turbulence models. The k-ω SST model gave the lowest maximum y+ value of 272.2 followed by k-ω model with 282.6 and k-ε model with 343.1. The higher maximum for the k-ε model shows a larger wall distance at some parts on the airfoil, which may have influenced its predicted of near-wall flow and contributed to its inconsistent lift and drag results. But these values only represent the maximum y+ recorded for each simulation and not the average or full distribution, so they are not enough to independently verify the suitability of the boundary-layer mesh.

6. Conclusion

The effect of angle of attack on the aerodynamic performance of a NACA 2412 airfoil has been investigated by using the k-ε, k-ω, and k-ω SST turbulence models in this study. The results indicated that the choice of turbulence model had a substantial impact on the predicted lift, drag, and lift-to-drag ratio. The k-ω SST turbulence model provided the most physically consistent lift trend and the closest agreement with the experimental data, although it generally underpredicted the experimental lift coefficients. The k-ω model also predicted an overall increase in lift, although the lift coefficient decreased slightly from 0.399 at 4 degrees to 0.397 at 6 degrees. Drag generally increased with angle of attack, but the lift-to-drag ratio showed that an increase in lift doesn’t automatically yield better aerodynamic efficiency, or lift-to-drag ratio. The results as a whole indicate that the k-ω SST was the best among the three turbulence models for predicting the aerodynamics of a NACA 2412 airfoil under the tested conditions. Further work may include mesh refinement and comparison of turbulence models with results from a different airfoil.

7. References

[1] Abbott, I. H., & Von Doenhoff, A. E. (1959). *Theory of wing sections: Including a summary of airfoil data*. Dover Publications.

[2] Akgümüş Gök, D., & Alnimer, K. (2024). Characterization of NACA 2412 and NACA 4412 airfoils: Effects of angle of attack on aerodynamic coefficients. *Journal of Thermal Engineering, 10*(6), 1524–1538. https://jten.yildiz.edu.tr/storage/upload/pdfs/1731578878-en.pdf

[3] Bourisli, R. I., & Hamadeh, F. Z. S. (2020). *Optimizing NACA airfoil thickness function parameters for maximum lift-to-drag ratio*. In *AIAA SciTech 2020 Forum*. https://doi.org/10.2514/6.2020-1297

[4] Launder, B. E., & Spalding, D. B. (1974). The numerical computation of turbulent flows. *Computer Methods in Applied Mechanics and Engineering, 3*(2), 269–289. https://doi.org/10.1016/0045-7825(74)90029-2

[5] Menter, F. R. (1994). Two-equation eddy-viscosity turbulence models for engineering applications. *AIAA Journal, 32*(8), 1598–1605. https://doi.org/10.2514/3.12149

[6] Prabhakar, A., & Ohri, A. (2013). *CFD Analysis on MAV NACA 2412 Wing in High Lift Take-Off Configuration for Enhanced Lift Generation*. Journal of Aeronautics & Aerospace Engineering, 2(5), 125. DOI: 10.4172/2168-9792.1000125.

[7] Seetharam, H. C., Rodgers, E. J., & Wentz, W. H., Jr. (1977). *Experimental studies of flow separation of the NACA 2412 airfoil at low speeds* (NASA Contractor Report NASA-CR-19950002355). Wichita State University, Aeronautical Engineering Department.

[8] Versteeg, H. K., & Malalasekera, W. (2007). *An introduction to computational fluid dynamics: The finite volume method* (2nd ed.). Pearson Education.

[9] Wilcox, D. C. (2006). *Turbulence modeling for CFD* (3rd ed.). DCW Industries.